JOC The Journal of Organic Chemistry

Article

pubs.acs.org/joc

Synthesis, Thermal Stability, Biophysical Properties, and Molecular Modeling of Oligonucleotides of RNA Containing 2′-*O*-2-Thiophenylmethyl Groups

Joseph C. Nguyen, Yannick Kokouvi Dzowo, Carly Wolfbrandt, Justin Townsend, Stanislav Kukatin, Haobin Wang, and Marino J. E. Resendiz*

Department of Chemistry, University of Colorado Denver, Science Building 1151 Arapahoe Street, Denver, Colorado 80204, United States

Supporting Information

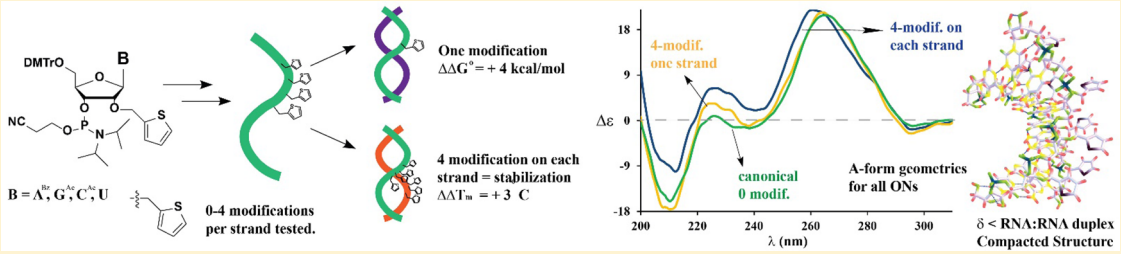

ABSTRACT: Dodecamers of RNA [CUACGGAAUCAU] were functionalized with C2′-*O*-2-thiophenylmethyl groups to obtain oligonucleotides **10**−**14** and **17**. The modified nucleotides were incorporated into RNA strands via solid-phase synthesis. The biophysical properties of these ONs were used to quantify the effects of this modification on RNA:RNA and RNA:DNA duplexes. A combination of UV−vis and circular dichroism were used to determine thermal stabilities of all strands, which hybridized into A-form geometries. Destabilization of the double stranded RNA was measured as a function of number of consecutive modifications, reflected in decreased thermal denaturation values (ΔT_m, ca. 2.5−11.5 °C). Van't Hoff plots on a duplex containing one modification (**10**:**15**) displayed a ca. $\Delta\Delta G°$ of +4 kcal/mol with respect to its canonical analogue. Interestingly, hybridization of two modified strands (**13**:**17**, containing a total of eight modifications) resulted in increased stability and a distinct secondary structure, reflected in its CD spectrum. Molecular modeling based on DFT calculations shed light on the nature of this stability, with induced changes in the torsional angle δ (C5′-C4′-C3′-O3) and phosphate-phosphate distances that are in agreement with a compacted structure. The described synthetic methodology and structural information will be useful in the design of thermodynamically stable structures containing chemically reactive modifications.

INTRODUCTION

RNA and DNA can be synthetically modified to obtain functional oligonucleotides (ONs) with a wide range of applications that include nanomaterials,[1] gene therapy,[2] structure analysis probes,[3] or sensing technologies[4] among many others. Functionalization can be carried out at either the nucleobase or at the ribose ring and with varying number of modifications per strand, including wholly modified ONs. Examples that illustrate the applications and advantages of chemically modified ONs (see Figure 1 for the structural representation of selected cases) rely on the incorporation of groups with spin-label properties[6] or fluorophores[7,8] to monitor structural changes in RNA via EPR spectroscopy[9,10] or fluorescence.[11] More related to this work are the use of small aromatic molecules as modifications at the C2′-*O*-position of the ribose unit. For example, Hrdlicka and co-workers have effectively shown the use of pyrene to build ONs of DNA that serve as invader duplexes on double-stranded DNA (dsDNA).[12] Another strategy relies on the use of functional groups such as methyl, ethyl esters, carbamoyl, methoxyethyl, fluoro, or nitrile, due to their induced properties, e.g., increased thermal and chemical stability and retention of fidelity toward Watson−Crick base pairing interactions, as well as potential applications in antisense technologies.[13−16] Another important family of compounds that involve modification at the C2′-*O*-position are locked nucleic acids (LNAs) containing pyrene,[17,18] coronene,[19] or groups that introduce the possibility for subsequent functionalization[20] as tools to detect cellular RNA via increased fluorescence and photophysical efficiencies. In this work, we used a 2-thiophenylmethyl functional group to modify dodecamers of RNA at the C2′-*O*-position (Figure 1, box) in our initial efforts to develop biopolymers with potential applications as probes to control structure and function of RNA. We reasoned that thiophene was an attractive target based on (1) its size, which prevents major structural disruptions; (2) wide use in other fields such as materials science, thus expanding its potential reactivity and ability for

Received: July 5, 2016
Published: September 1, 2016

DOI: 10.1021/acs.joc.6b01615
J. Org. Chem. 2016, 81, 8947−8958

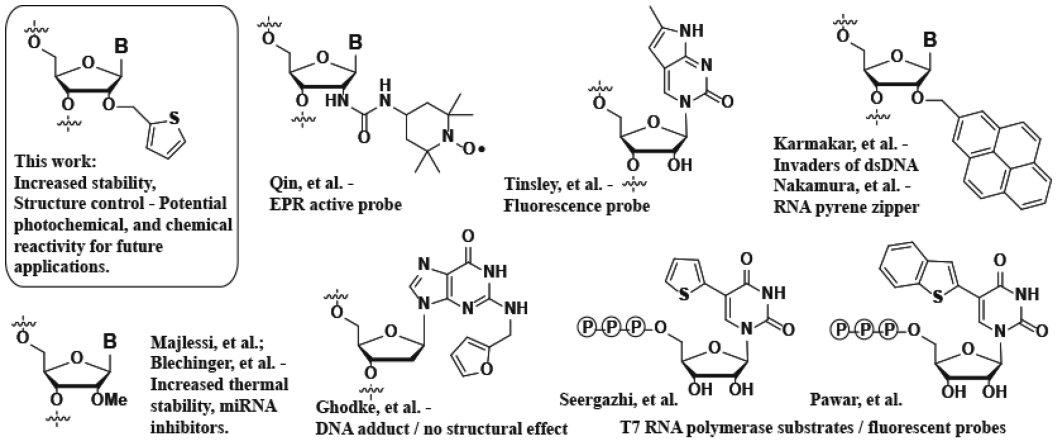

Figure 1. 2-Methylthiophene was used as the modification in this work. Other relevant examples illustrating modification at the C2′-position as well as the use of thiophene at the nucleobase are shown and mentioned in the Introduction.

Scheme 1[a]

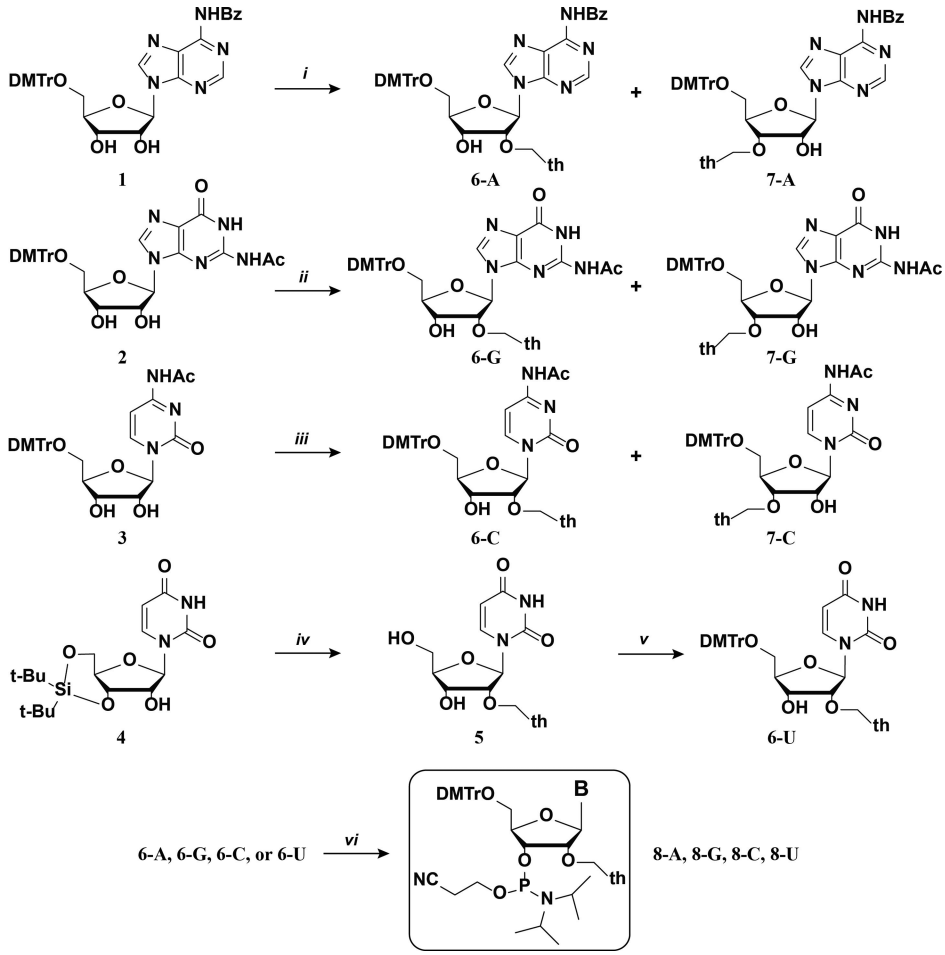

[a](i) LiHMDS, 2-chloromethylthiophene, THF/DMSO; (ii) KH, 2-(chloromethyl)thiophene, THF/DMSO; (iii) NaHMDS, 2-(chloromethyl)-thiophene, THF/DMSO; (iv) NaHMDS, 2-(chloromethyl)thiophene, THF/DMSO; then 3HF·Et_3N, THF; (v) DMTrCl, pyr.; (vi) *N*,*N*′-Diisopropylamino cyanoethyl phosphonamidic-Cl, DCM, DIPEA.

additional probe-functionalization; and (3) photophysical behavior (different absorption wavelength, λ_{max}, from that of the nucleobases), making these probes bioorthogonal. Combined, we are interested in the use of thiophene and thiophene-derivatives to induce intrastrand reactivity that clip the strands of interest to yield different structural arrangements, e.g., circular RNAs, without losing its original Watson−Crick basepairing ability. It is expected that the induced reactivity and structure changes will yield strands of RNA that will enable the control of function, potentially with antisense properties. To this end, we explored the effect of 2-thiophenylmethyl groups on single stranded RNA and duplex structures of RNA:RNA

DOI: 10.1021/acs.joc.6b01615
J. Org. Chem. 2016, 81, 8947−8958

and RNA:DNA hybrids via UV−vis and CD spectroscopy. Furthermore, electronic structure calculation employing density functional theory (DFT) was used to determine the nature of the structural changes imposed by this modification. The experimental data and modeling presented herein are guiding our efforts to manipulate the structure and function of RNA by functionalizing its backbone with groups that are responsive to chemical and/or photochemical stimuli.

Some examples in literature with a close relationship to this work include reports by Nakamura and collaborators in their use of the 1-pyrenylmethyl functional group as a modification, to whom we make reference in detail throughout the discussion.[5] Thiophene represents the basis of the modification in this work and has been previously used in different contexts to adorn ONs of DNA and/or RNA for different applications. Examples include ONs as sequence-dependent fluorescent probes[21] at the C5-position of deoxyuridine in DNA as well as on the C6-position of adenosine in RNA.[22] Furthermore, C5-thiophenylmethyl substituted uridine has been incorporated efficiently into RNA using T7 RNA polymerase,[23] with a larger group such as the C5-benzothiophenylmethyl group functioning as a good substrate of the same polymerase.[24] Other modifications that occur naturally include the methylfurfuryl moiety, which was synthesized, incorporated, and tested on oligonucleotides of DNA recently.[25] This modification was installed at the N2-position of guanosine, and the corresponding thermodynamic parameters showed destabilization with depressed T_m values. These examples indicate that the size of thiophene can be compatible with some biological processes, which makes it an attractive oligonucleotide probe.

RESULTS

Synthesis of Modified Monomers. Different strategies can be pursued in the synthesis of oligonucleotides of RNA modified with aromatic groups at various positions. These include addition onto the nucleobase (via Stille cross-coupling on solid support) through the use of iodo precursors that lead to furyl-, thienyl-, or benzothienyl-functionalized ONs;[26] or via alkylation of the free nucleobase, albeit at the expense of decreased selectivities and/or yields. In this work, the four canonical nucleosides, guanosine (G), adenosine (A), uridine (U), and cytidine (C), were functionalized at the C2′-*O*-position using reaction conditions that varied with nucleoside, resulting in good selectivities (with the exception of cytidine) and fair to good yields. With regards to the chosen modification, we envisioned using a group that would minimize changes in the canonical secondary structures and with photophysical properties that would enable our ability to characterize and quantify its effects. We decided to use 2-methylthiophene as a substituent, based on its small size, photophysical behavior ($\lambda_{max} \neq 250-280$ nm), and potential for reactivity under a variety of conditions, e.g., thermal, photochemical, chemical,[27] for future applications. As a way to facilitate the synthesis of the final phosphoramidites, necessary intermediates in nucleic acid solid-phase synthesis, we envisioned protecting each nucleoside with groups amenable for solid-phase synthesis prior to their functionalization (Scheme 1).

In light of previous results that use nitrobenzyl bromide reagents to functionalize the hydroxyl groups,[28,29] we attempted the bromination of 2-thiophenemethanol in the presence of phosphorus tribromide.[30] Unfortunately, this reaction resulted in polymerization and other unidentified byproducts, while the use of a tosyl-group impacted its subsequent reactivity negatively. Therefore, we prepared the alkylating agent "2-(chloromethyl)thiophene" from the reaction of 2-thiophenemethanol and thionyl chloride[31] and settled for this electrophile as the choice for our experiments, which required the use of solvent mixtures (THF/DMSO) for the substitution reactions to proceed in all cases (reactions carried out using the free nucleosides led to low yields). As depicted in Scheme 1, this strategy was fruitful in the cases of A, G, and C as follows: (1) Adenosine was benzoylated and tritylated under standard conditions to yield nucleoside **1**, which was in turn alkylated in the presence of lithium hexamethyldisilylazide (LiHMDS) and 2-(chloromethyl)thiophene to obtain a mixture of regioisomers, with the C2′-isomer **6-A** as the major product; (2) *N*-Acetylated guanosine was tritylated leading to protected nucleoside **2**, then treated with potassium hydride (KH) and 2-(chloromethyl)thiophene to yield the C2′-alkylated nucleoside **6-G** as the major product; and (3) Cytidine was acetylated and tritylated to obtain the corresponding nucleoside **3**, followed by its reaction with 2-(chloromethyl)thiophene in the presence of NaHMDS, which led to a mixture of regioisomers with the C2′-functionalized material **6-C** as a minor constituent within the mixture of obtained products. Uridine was an exception in this strategy in that its derivatization started with the di-*t*-Butylsilyl protected analogue **4** followed by alkylation in the presence of NaHMDS and 2-(chloromethyl)thiophene. Subsequent deprotection using hydrogen fluoride yielded the expected C2′-alkylated derivative **5**. The modified nucleoside was then tritylated to obtain the desired precursor **6-U**. We found that the selectivity and yield to obtain the desired products varied under different conditions and was highly dependent on the nature of each nucleobase, e.g., treatment of tritylated uridine with LiHMDS, NaHMDS, NaH, or KH led to a complex mixture that included N-alkylation products in each case; treatment of protected guanosine **2** with LiHMDS or NaHMDS led to N-alkylation as well as bis-addition products; or treatment of DMT-C^{Ac} **3** with NaHMDS was unreactive, while NaH or KH led to bis-addition or C3′-alkylated regioisomer **7-C** as the major constituent in the reaction. Regiochemistry of all isomers (**6-A**, **6-G**, **6-C**, **6-U**) was confirmed via homonuclear 2-D-NMR (COSY), which served to identify a correlation between the C2′-H and the C1′-H followed by correlation between the OH and the C3′-H. The same analysis was carried out with the C3′-regioisomers (**7-A**, **7-G**, **7-C**), in which a correlation between the C2′-H and the C1′-H along with that between the OH and the C2′-H was consistent with our proposed structures. Some interesting differences in the spectroscopic and physical properties between regioisomers **6** and **7** that are worth mention and that were consistent regardless of the identity of the nucleobase are as follows: (1) chromatographically, all C2′-*O*-alkylated regioisomers **6** displayed a larger response factors (using silica as the adsorbent) than the C3′-isomers **7**; (2) in ^{1}H NMR, the diastereotopic C5′-H signals corresponding to the C2′-functionalized nucleosides **6** coalesced or had a smaller $\Delta\delta$ than those obtained for the C3′-analogues **7**; (3) the same effect was observed with the methylene protons on the thiophene unit, where a higher resolution was observed in all cases for nucleoside **7**; and (4) all C2′-OH signals appeared consistently at higher field than the corresponding C3′-OH. In addition, the appearance of the amido N−H signals (δ 9−11, $CDCl_3$) was clearly observed in all spectra with the exception of the *N*-alkylated substituents (not reported or used herein).

DOI: 10.1021/acs.joc.6b01615
J. Org. Chem. 2016, 81, 8947−8958

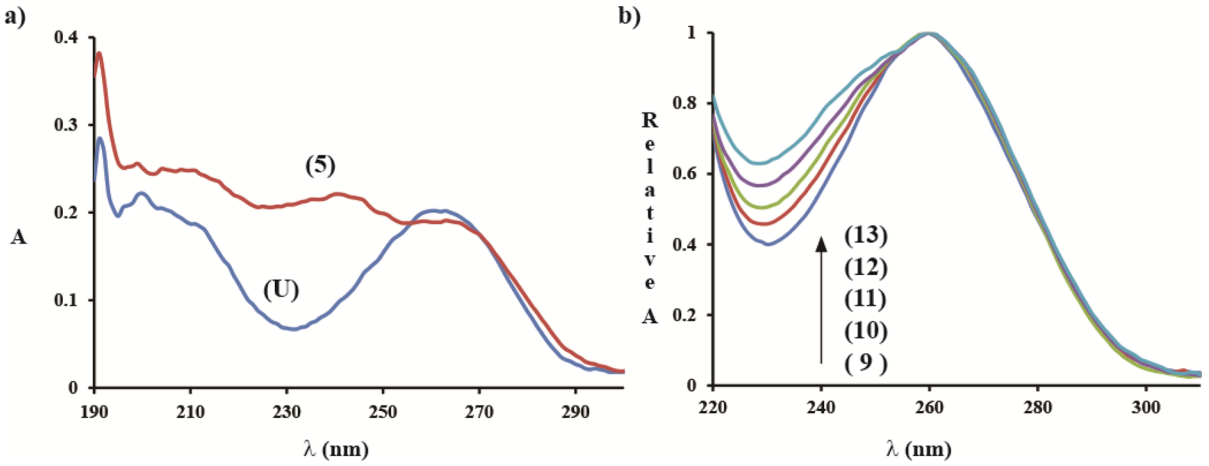

Figure 2. UV−vis spectra corresponding to (a) uridine (**U**) compared to modified uridine (**5**) in water and (b) normalized spectra of ss-RNA strands **9** → **13** taken in water.

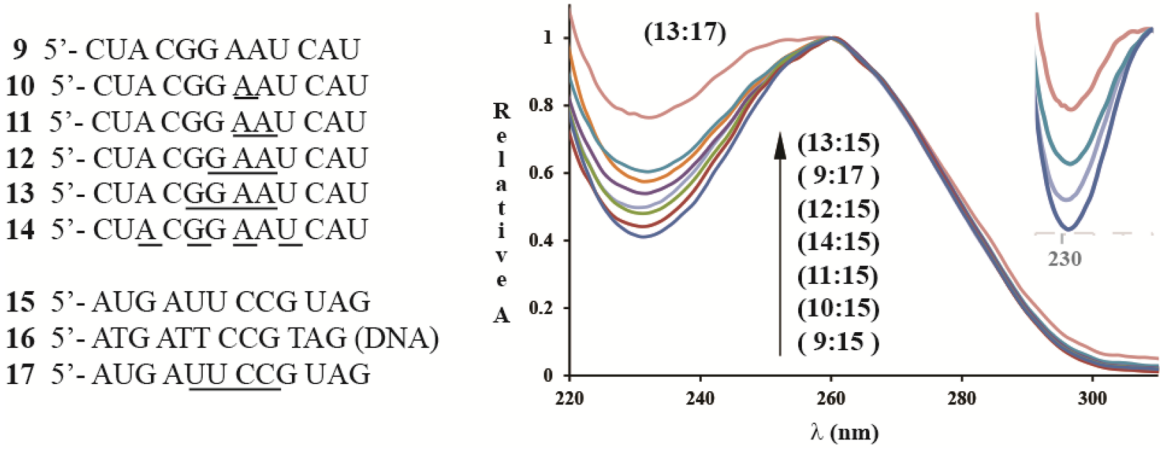

Figure 3. Oligonucleotide sequences used in this study with underlined letters representing modified positions (left). Normalized UV−vis spectra corresponding to each RNA:RNA homoduplex structures (right). Region corresponding to thiophene absorption band shows decreasing extinction coefficient at ca. 230 nm with the following trend: **13**:**17** → **13**:**15** → **14**:**15** → **9**:**15** (inset, highest → lowest ε).

Overall, the developed methodology provides the target phosphoramidites **8** in yields that are comparable to those reported with the use of the unprotected nucleosides.[32]

UV−Vis and CD Spectroscopy. A comparison of the UV−vis spectrum for uridine with that of the C2′-*O*-functionalized analogue **5** clearly shows the photophysical differences induced by the presence of one thiophene ring. The spectrum for nucleoside **5** displayed a band with a λ_{max} at 262 nm (ε, 10 500) that can be assigned to the nucleobase along with a band showing higher absorption at a λ_{max} of 240 nm (ε, 12 250), corresponding to the thiophene unit (Figure 2a). Taking into consideration the differences in ε_{260} values for A (15 000), G (14 000), C (8700), and U (9800),[33] it is reasonable to expect that in an oligonucleotide (single stranded form) containing equal number of nucleotides and thiophene modifications that the peak intensities at both λ_{max} 260 and 240 will display comparable extinction coefficients.

Each modified monomer of **6** was phosphitylated under standard conditions leading to their corresponding phosphoramidites **8**-**A**, **8**-**G**, **8**-**C**, and **8**-**U** in good yields. All products led to efficient couplings (>97%) upon their incorporation into oligonucleotides of RNA via solid-phase synthesis. We decided to test the effect of this modification on homoduplex (RNA:RNA) and heteroduplex (RNA:DNA) structures using 12-mers containing as many as four thiophene units per strand. The design of the ONs was such that their length and sequence ensured a minimum of one turn and without the possibility for formation of other thermodynamically stable structures such as self-dimers, hairpins, or slip-duplexes. A combination of UV−vis and circular dichroism (CD) were used to establish the photophysical behavior and structural aspects of the modified oligomers, respectively. The sequence of the ONs that we studied is shown on Figure 3 and differ by the number of modifications increasing from zero to four (**9** → **13**) with strand **14** containing four modifications every other nucleotide. Oligomers **15**, **16**, and **17** correspond to the RNA, DNA and modified RNA complementary strands, respectively. In agreement with an incremental number of thiophene rings within the strands, UV−vis spectroscopy of single stranded coils **9** → **13** displayed a hyperchromic shift at ca. λ_{max} = 230 nm (Figure 2b). The same pattern was observed upon comparison of ONs **15** with **17** and **9** with **14** (see SI). We then proceeded to hybridize the ONs with their corresponding complementary strands and measured their UV−vis response in buffered solutions at neutral pH. As expected from formation of a duplex structure, a hyperchromic shift was observed in all cases with

DOI: 10.1021/acs.joc.6b01615
J. Org. Chem. 2016, 81, 8947−8958

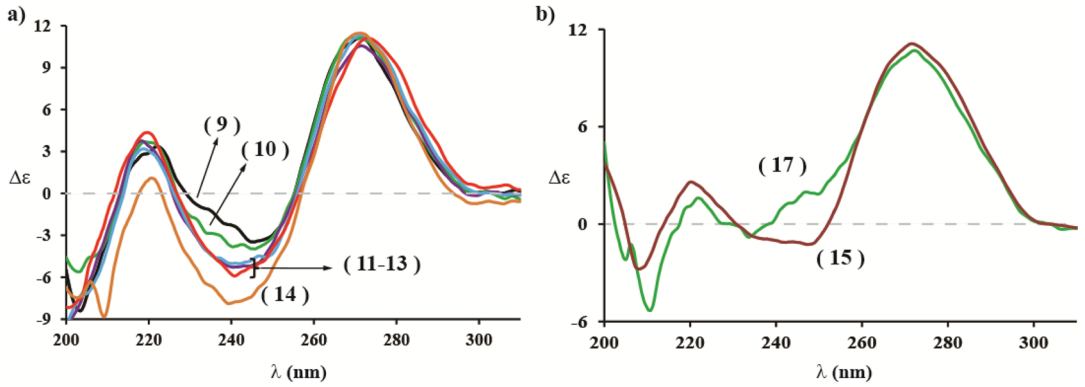

Figure 4. CD spectra of single stranded RNAs **9**−**14** (a) and **15**, **17** at [5 μM] in phosphate buffered solutions (pH 7.2).

respect to their corresponding single stranded forms. As illustrated on Figure 3, a hyperchromic shift in the 220−250 nm region was observed, consistent with a higher number of thiophene rings present in the strand. Since the largest difference in the ε values between modified and canonical ONs was observed at ca. 230 nm (Figures 2a,b and 3), we decided to use this value to describe the spectroscopic changes induced by the modification. Interestingly, clear differences were observed on duplexes containing four thiophene units as follows: (1) Comparison between **13**:**15** and **14**:**15** displayed a hypochromic shift that suggests that positioning of the modifications in a consecutive manner results in a degree of cooperativity between the thiophene units on the strand; (2) The observed difference between **13**:**15** and **9**:**17**, with the latter having a lower ε_{230} value, suggests that purine rich sequences containing modifications result in stronger interactions between the thiophene units, compared to their pyrimidine modified analogue; and (3) Duplex **13**:**17** containing eight thiophene units total, displayed a ε_{230} value which was approximately double the value of that corresponding to duplex structure **13**:**15**.

We then used circular dichroism (CD) to obtain information about the structure and stability of the designed RNA strands. CD spectra of all ONs in their single stranded form lacked the features that are expected to appear upon formation of secondary structures (Figure 4). While both the nucleobases and modifications are planar and achiral as single units and thus unresponsive to circularly polarized light, their linkage to the ribose unit results in ellipticity that increases as a function of ON length. Wavelengths where a chromophore absorbs light give rise to distinct patterns, albeit with diminished ellipticity compared to those forming a secondary structure. As such, a dominant band with positive ellipticity at ca. 270 nm was observed in all cases, arising from the presence of the nucleobases without the hyperchromicity expected from π−π-stacking occurring on duplex samples. Taking into consideration that the λ_{max} in the UV−vis spectra of the thiophene rings is observed at ca. 220−240 nm, we decided to inspect this region more closely. Comparison of the spectra corresponding to ONs **9**−**13** shows a hypochromic shift as a function of increasing number of modifications (Figure 2a), with modified ONs **11**−**13** following identical patterns. Interestingly ON **14**, with four modifications placed every other nucleobase, shows a band with lower ellipticity at ca. 240 and 225 nm, suggesting a different structural arrangement for this ON. Comparison of the complementary strands **15** and **17** yielded the following observations (Figure 2b): (1) hyperchromic and hypochromic shifts were observed at ca. λ 240 and 210 respectively; and (2) the trend is opposite of that observed from complementary strands **9**−**14** in both cases. The observations summarized on Figure 2 reflect the sensitivity of CD toward structure and sequence[34] and some examples that highlight this phenomenon are discussed in the Discussion section.

ONs **9**−**14** and **17** were then hybridized with their complementary strands in saline phosphate buffered solutions (pH 7.2) and the resulting structures were characterized via CD. All samples displayed features consistent with A-form geometries clearly evidenced on the canonical duplex **9**:**15** by the concomitant appearance of a band with negative ellipticity at 210 nm along with a hyperchromic shift on the band at 260 nm (Figure 5).[35] CD spectra of the modified ONs **10**−**14**:**15** displayed similar features to their canonical analogue and only a slight hyperchromic shift as a function of increased number of modifications was observed in the 220−250 nm range. These results suggest that all strands have similar structural arrangements. In contrast with the single stranded results, no clear structural differences were observed between duplex samples containing four thiophene units consecutively (**13**:**15**) or in an intercalated fashion (**14**:**15**). Assignment of the bands corresponding to the thiophene units became unambiguous upon comparison of these spectra with the double stranded sample containing eight thiophene units (**13**:**17**), where the intensity in the bands at ca. 225 and 240 nm experienced a hyperchromic effect. This observation suggests that the thiophene units are contributing to the overall formation of

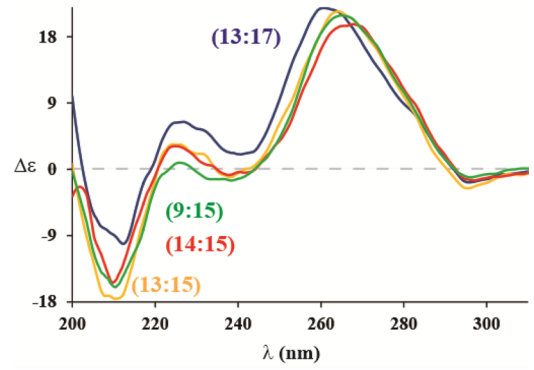

Figure 5. CD spectra of selected structures showing A-form geometries in all cases with some differences (see text) at [ds-RNA] = 2 μM.

DOI: 10.1021/acs.joc.6b01615
J. Org. Chem. 2016, 81, 8947−8958

Table 1. T_m Values of Homo- and Heteroduplex of Canonical and Modified RNAs[a]

RNA:RNA	T_m	ΔT_m	RNA:DNA	T_m	ΔT_m	homo-hetero $\Delta\Delta T_m$
9:15	66 ± 0.1	–	**9:16**	49.4 ± 0.4	–	–
10:15	60.4 ± 0.4	−5.6 ± 0.4	**10:16**	47.3 ± 0.1	−2.1 ± 0.4	−3.5 ± 0.6
11:15	61.6 ± 0.3	−4.4 ± 0.3	**11:16**	43.1 ± 0.2	−6.3 ± 0.4	+1.9 ± 0.5
12:15	61.9 ± 0.1	−4.1 ± 0.1	**12:16**	42.4 ± 0.6	−7 ± 0.7	+2.9 ± 0.7
13:15	57.1 ± 0.9	−8.9 ± 0.9	**13:16**	40.3 ± 0.1	−9.1 ± 0.4	+0.2 ± 1
14:15	55.7 ± 0.7	−10.3 ± 0.7	**14:16**	39.7 ± 0.5	−9.7 ± 0.6	−0.6 ± 0.9
9:17	62.6 ± 0.6	−3.4 ± 0.6				
13:17	69.6 ± 0.6	+3.6 ± 0.6				

[a] ΔT_m indicates the difference when compared to the canonical analogue. $\Delta\Delta T_m$ (homo-hetero) indicates the difference in ΔT_m between homo- and heteroduplex structures. All T_m values were obtained via CD recorded at 210 nm. The error represents that of experiments carried out in triplicate. All samples were prepared in 5 mM $MgCl_2$, 1 mM Sodium phosphate, 10 mM NaCl, pH 7.3.

the final secondary structure with added cooperativity between the thiophene units present on both strands. Other spectroscopic differences induced by the presence of thiophene units on each strand include the hyperchromic shift in the band at ca. 210 nm along with a hypsochromic shift in the major band with positive ellipticity (265 → 260 nm). Experiments carried out on the RNA:DNA heteroduplex structures (**9**–**14**:**16**) displayed a similar pattern to that observed for the corresponding RNA:RNA homoduplex samples.

Measurement of T_m. To test the effect of the modifications on the thermal stability of the duplex structures, we determined the thermal denaturation transitions (T_m) of all ONs via CD. All measurements collected on homo- and heteroduplexes were carried out by recording the change in ellipticity at 210 nm as a function of increasing temperature. We decided to use this wavelength because of its exclusive appearance upon formation of an A-form duplex, with both canonical and modified duplex strands displaying a biphasic behavior that was independent of pH or salt concentration (Na^+ or Mg^{2+}) and with a minor transition observed between ca. 20−35 °C along with a single major transition well above this temperature (see SI). The T_m values reported in Table 1 correspond to the major and most significant phase transition. Destabilization as a function of number of modifications, evidenced from the drop in the measured T_m values, was generally observed excluding that when both strands are modified (**13**:**17**). While the relationship between thermal destabilization and number of thiophene units follows a relatively linear trend in the case of the RNA:DNA heteroroduplex structures (with a small difference observed between the bis- and tris-modified strands **11**:**16**/**12**:**16**) the data obtained for the homoduplex analogous complexes is not as clear. That is, while addition of one thiophene unit does destabilize the homoduplex, the presence of two or three modifications (**11**:**15** and **12**:**15**) results in increased stabilization with respect to the monomodified **10**:**15**. Also, while one modification disrupts the RNA:RNA hybrid more than the RNA:DNA analogue by ca. 3.5 °C, the presence of four modifications (consecutive or intercalated) results in the same destabilizing effect. To ensure that the choice in the wavelength at 210 nm is a reliable strategy we carried out two additional measurements for each sample: (1) we measured the thermal denaturation transitions at 270 nm via CD; and (2) we used the obtained optical dispersion (OD 260/280) of the RNA:RNA duplexes to determine the melting transitions.[36,37] Gratifyingly, both measurements were in close agreement with the values displayed on Table 1, thus validating the approach taken herein (see SI for all the obtained data).

To quantify the observed destabilization effect of one thiophene ring, we measured the thermodynamic parameters for RNA:RNA duplexes **9**:**15** and **10**:**15** by deriving the corresponding Van't Hoff plots[38] (assuming a two-state model), which, resulted in a drop in the free energy of ca. 8.1 ± 3.9 kcal/mol (Table 2). This is in the range of the energy

Table 2. Thermodynamic Parameters Were Derived from Van't Hoff Plots of $1/T_m$ vs $\ln(C_t/4)$ at 25° C[a]

RNA:RNA	$\Delta G°$ (kcal mol^{-1})	$\Delta H°$ (kcal mol^{-1})	$\Delta S°$ (cal mol^{-1} K^{-1})
9:**15**	−29.3 ± 2.4	−185 ± 21	−523 ± 64
10:**15**	−21.2 ± 3.1	−118 ± 27	−323 ± 79
ΔΔ values	+8.1 ± 3.9	+68 ± 34	200 ± 102

[a] All samples were prepared in 5 mM $MgCl_2$, 1 mM Sodium phosphate, 10 mM NaCl, pH 7.3 and carried out in duplicate. [RNA] ranged between 0.5 and 20 μM.

difference observed in a recent study carried out on 14-mers of RNA functionalized at a single site with a 2′-trifluoromethylthio-modification, which displayed duplex destabilization of ca. $\Delta\Delta G°$ −7.6 kcal mol^{-1}/$\Delta\Delta H°$ −40 kcal mol^{-1} with respect to its canonical analogue.[39]

Furthermore, analysis of duplexes **13**:**15** and **9**:**17** shows that the thermal stability imposed by the modifications depend on the nature of the nucleobase, with modified purines resulting in larger destabilization than pyrimidine nucleotides containing thiophene units. Also, duplex **14**:**15** which contains four intercalated modifications resulted in a larger destabilization than that of both duplexes containing consecutive thiophene units (**13**:**15**/**9**:**17**) with a $\Delta\Delta T_m$ value of ca. 1.4 ± 1.3° and 6.9 ± 0.9 °C. This result also points to a position dependent destabilization and suggests that higher ordered structures may be achieved upon placement of this modification on adjacent sites. Interestingly, hybridization of both functionalized ONs **13** and **17** resulted in stabilization of the corresponding duplex, reflected in the obtained higher T_m values with respect to its canonical analog (**9**:**15**, ca. ΔT_m + 3.6 °C). The increased T_m suggests a significant structural effect imposed by the presence of thiophene units on complementary strands, resulting in added stability despite the increased number of thiophene rings to a total of eight.

In lieu of this result we took a closer look at the behavior of the duplex samples containing four modifications on each strand (**13**:**17**). As depicted on Figure 6, the bands with ellipticity at 210, 225, 240, and 260 nm are affected significantly upon heating of samples containing the hybrid structure. As in the other samples, the band at 210 nm (assigned to formation

DOI: 10.1021/acs.joc.6b01615
J. Org. Chem. 2016, 81, 8947−8958

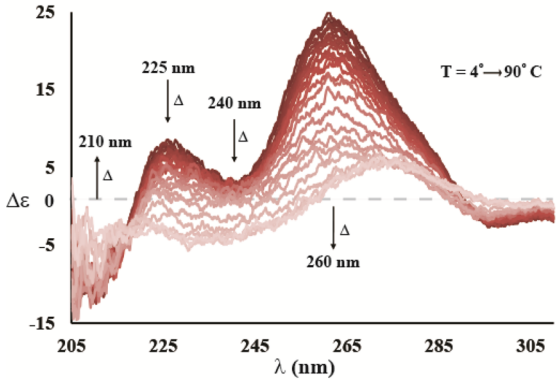

Figure 6. CD spectra of duplex **13**:**17** acquired every 2 to 4 °C on heating the sample from 4 to 90 °C at [RNA] = 3 μM. Data shown corresponds to raw data after 2 accumulations at each temperature.

of an A-form duplex) experiences an increase in ellipticity while the band at 260 nm (a feature of the ordered $\pi-\pi$ stacking between nucleobases) decreases in intensity along with a bathochromic shift (ca. 260 → 270 nm). Interestingly, the bands at 225 and 240 nm (assigned to the thiophene units in this work) experienced a change in sign on the ellipticity. Furthermore, T_m measurements recorded at these wavelengths ($T_{m\text{-}225nm}$ = 66.4 °C, $T_{m\text{-}240nm}$ = 67.5 °C) were in close agreement to those obtained at 210 nm (Table 1). Assignment of these bands to the thiophene units was confirmed with the lack of ellipticity variations at these wavelengths upon recording CD spectra of the canonical duplex **9**:**15**, where as expected, only changes in the bands at 210 and 260 nm were observed (SI). These observations validate the use of thiophene (and potentially other groups that absorb at different regions) as a tool to detect thermodynamic variations at various wavelengths and confirms that the presence of these aromatic rings are an intricate part that directly affect the structure, in this case by adding stability.

Molecular Modeling: Computational Methods. To address the nature of the stabilizing effect of RNA duplex **13**:**17**, we carried out electronic structure calculations that compare this complex with its canonical analogue using the density function theory (DFT). We used a duplex conformed by two 6-mers with and without modifications positioned in the middle of each strand (RNA **18**:**19**/**20**:**21**) as model. These sequences were chosen to ensure duplex formation as the only thermodynamically stable structure and to keep purine/pyrimidine rich regions in addition to pyrimidines flanked by purines (and vice versa). All calculations were performed using the quantum chemical program package Gaussian 09.[40] The B3LYP hybrid functional, which includes the Becke three-parameter exchange and the Lee, Yang, and Parr correlation functional, was used in the electronic structure calculation. The 3-21G* basis set in Gaussian 09 was used in the investigation. An implicit solvent approach, the polarizable continuum model (PCM) approach,[41−43] was used to model the solution environment. Geometry optimizations were carried out for the duplex models with the PCM approach, which gave much more realistic, compact structures than those relaxed in gas phase. To gauge the robustness of the results, test calculations were also performed for smaller duplex models with larger basis sets and with empirical dispersion corrections. The qualitative conclusions were not changed upon using these different approaches. The Cartesian coordinates of the optimized structures are given in the Supporting Information (SI).

To further quantify the obtained structures, we measured the torsion angles χ (glydosidic dihedral angle between sugar and nucleobase) and δ (backbone dihedral angle along the ribose ring) from the optimized structures. Gratifyingly, torsional angles obtained for both canonical (**20**:**21**) and modified (**18**:**19**) models clustered in the region corresponding to A-form geometries ($-140° > \chi < -170$ and $65° > \delta < 100°$), in agreement with CD data obtained experimentally. Further analysis indicates that the structure of the modified duplex is constituted by a more compact helix than its canonical analogue as follows (Figure 7): (1) the measured angles display a pattern where the majority of the nucleotides in the modified version have shorter rotational angles (δ °); (2) comparison of the phosphate-phosphate distances on both structures showed that those on the modified structure **18**:**19** are generally shorter

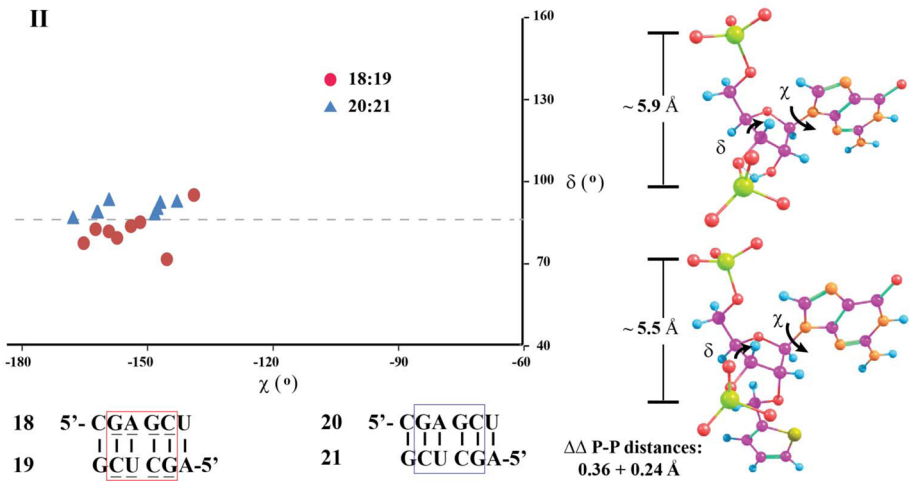

Figure 7. Sequence of ONs **18**:**19** and **20**:**21**, where the underlined nucleotides represent 2′-*O*-thiophenylmethyl modified positions and the area within the square represents the area of interest. A plot displaying the (χ, δ) angle covariance matrix is shown with modified duplex at lower dihedral angle δ within quadrant II of the Cartesian coordinate system (left). Monomers taken from the calculations (deleting all other atoms from the duplexes) are used to depict the reference torsion angles χ (pyrimidines: O4′−C1′−N1−C2; purines: O4′−C1′−N9−C4) and δ (C5′−C4′−C3′−O3) (right).

DOI: 10.1021/acs.joc.6b01615
J. Org. Chem. 2016, 81, 8947−8958

with differences ranging between 0.1 and 3.7 Å (see SI for full table). It is then reasonable to conclude that placing the methylthiophenyl modification imparts a change in the rotational angle (δ) that results in the observed compactness, and is the root of the observed stabilization. Comparison of all other torsional angles (α, β, γ, ε, ζ, χ) between both models were within error of each other and in agreement with values corresponding to an A-form RNA duplex. Tables containing all measured values are included in the Supporting Information as well as side-by-side representations that compare both duplex structures.

Further analysis and validation of both structures focused on the conformation of the sugar ring, described by the pseudorotational angle (P).[44] Consistently, canonical duplex **20**:**21** displayed angles in the Northern region, N, of 9.6 ± 3.4°, values that are well in agreement with those expected for riboses in RNA adopting a standard C3′-*endo* conformation. On the other hand the same analysis for the modified duplex (**18**:**19**) led to a large standard deviation, 12.1 ± 10.1°. This prompted us to look at differences between pyrimidine- and purine-containing nucleotides, which lead to large variations in the latter of ca. 12.1 ± 2.3° and 11.6 ± 15.2° respectively. While there is a big discrepancy in the modified nucleotides, the values are still within the phase angle of the expected pseudorotational region for a C3′-*endo* pucker.

DISCUSSION

The thermodynamic stability and structural effects of ONs modified with methylthiophene units was described. The choice of this aromatic ring as the modification was made based not only on size but on its higher reactivity toward a variety of conditions that include thermal, photochemical, and chemical, for future studies. Gratifyingly, we successfully placed the target 2-methylthiophene unit on all four canonical nucleobases with the desired C2′-*O*- regioisomers set for their phosphytilation and subsequent incorporation into oligonucleotides of RNA. We tested the thermal stability and structural factors of the obtained modified ONs (**10**−**14** and **17**) on RNA:RNA homoduplex as well as RNA:DNA heteroduplex structures containing 1−4 modifications within one strand and up to eight modifications on two RNA complementary strands. The following important observations were made: (1) all structures hybridize into A-form duplexes; (2) addition of thiophene units destabilize the duplex structures as a function of added modifications on RNA:DNA heteroduplexes, while a different pattern (still with a destabilizing effect) was measured on the RNA:RNA homoduplex structures; (3) this effect is more pronounced on samples where the thiophene units are intercalated; (4) addition of thiophene units on both complementary strands increased the thermal stability upon formation of the duplex, where, the T_m can be measured at four distinct wavelengths (via CD); and (5) modeling showed that the root of the stabilization on **13**:**17** arises from the change in the backbone torsional angle (δ).

UV−vis spectroscopy of all ONs yielded an expected $\varepsilon_{225-240}$ increase as a function of thiophene rings added. Therefore, we focused on this region on the analysis via CD. Single stranded ONs showed differences between modified strands of **9** and complementary RNA **15**, with hypo- or hyperchromic shifts in the bands at 240 and 225 nm. This pattern is explained by the fact that CD is sensitive to sequence and modifications,[45] thus resulting in the observed changes in ellipticity. It is possible that this change arises from the fact that ON **9** has modified purines while ON **15** contains the thiophene rings on pyrimidine bases that may induce local variations in the C2′ versus C3′ endo sugar puckers or other interactions within the nucleobases and the modifications. The most interesting and relevant structural aspects were observed on homo- and heteroduplex samples containing the modifications in varying position and number. The higher T_m values obtained from RNA:RNA homoduplex compared to RNA:DNA heteroduplex structures (modified or unmodified) confirms the known higher compactness and rigidity in the former.[46] On this note, comparison of duplex structures (Figure 5) displayed a hypsochromic shift in the band at ca. 275−250 nm (**14**:**15** > **9**:**15** ≈ **13**:**15** > **13**:**17**), where the pattern is also in agreement with modified duplex **13**:**17** having a more compact structure. In addition, we quantified the destabilization of one thiophene unit to be in the range of $\Delta\Delta G°$ of 4 kcal mol^{-1} and rationalized that this was in agreement with values from other reported C2′-*O*-modifications.

As observed by Nakamura et al., the fact that the CD transitions are unchanged upon addition of each thiophene unit rules out the possibility of intercalation. Nakamura showed that pyrene units sit outside of the duplex in RNA, whereas intercalation is observed in the case of DNA.[47] Intercalation resulted in quenching of the fluorescence (corresponding to the pyrene rings) in DNA while an increased fluorescence was observed on ds-RNA. Nakamura also varied the number of methylpyrenyl units between zero and three using 20-mers of RNA and obtained a similar pattern as in this work, that is, increased destabilization of 4°, 5°, and 8 °C in the measured T_m with respect to canonical structures as a function of increased numbers of modifications.[48] These studies also showed that the pyrene was free of interactions with the nucleobase, an assumption that can be made in this work as well.

In agreement with a larger destabilization with purine-modified nucleotides, it has been reported of a similar effect on DNA B-form structures, where a sequence dependence in which flanking purines lead to greater duplex stabilization than pyrimidines was reported.[49] This observation is in agreement with the discrepancies obtained from modeling in which the purine containing nucleotides display a large range of the pseudorotational angle P.

In regards to the increased stabilization observed on duplex **13**:**17**, this seems to be a unique observation and different from results of Nakamura, where functionalization of both strands resulted in destabilization[50] or no change[51] upon functionalization of as many as ten nucleotides. One significant difference is the fact that in our case there is no canonical site between modifications; that is, the eight thiophene units on duplex **13**:**17** are on four consecutive sites on each strand and albeit a smaller aromatic ring than pyrene, it imparts a great deal of stability when present on these arrays. CD spectra obtained at different temperatures showed hypochromic shifts in the bands at 225 and 240 nm resulting in a change in sign in ellipticity, thus indicating that major local changes arising from the thiophene rings are induced upon melting. The sign change has been well characterized in dinucleotides of adenosine and was assigned to interactions between the nucleobases,[52] perhaps enhanced $\pi-\pi$ stacking in this case.

The molecular modeling supported the difference in stabilization energies that is provided by the thiophenes on both strands (ON **13**:**17**) and that relies on lower δ pseudorotation angles. Interestingly, among the artificial genetic polymers for which structural parameters are known[53] the

DOI: 10.1021/acs.joc.6b01615
J. Org. Chem. 2016, 81, 8947−8958

geometrical features match more closely to those observed from duplexes of two 2′-deoxy-2′-fluororibonucleic acid strands (FRNA).[54] However, contrary to the FRNA duplex, *P* values in our case showed that the C3′-*endo* sugar pucker is retained, thus providing a new geometrical/structural set for modified ONs.

CONCLUSION

Methodology that introduces 2-methylthiophenyl groups as a modification at the C2′-*O*-position on oligonucleotides of RNA was established. The effects of the thiophene rings in the context of structural and thermal variations were studied using RNA:RNA homoduplexes and RNA:DNA heteroduplexes as models. CD and UV−vis were used to establish these properties and determine structural and thermodynamic parameters of the obtained oligonucleotides. We found that this modification destabilizes double stranded samples incrementally as a function of number of modifications, with a measured value in the order of 4 kcal/mol when one modification is present. Positioning of the modification in an intercalated manner resulted in a larger destabilization than when they were located consecutively. Importantly, a significant thermal stabilization was observed on duplex samples in which complementary modified nucleobases impart stability to the structure via $\pi-\pi$ stacking interactions on the surface of the duplex. The use of CD shows that four different wavelengths can be used to measure thermal denaturation transitions, which expands the potential use of this spectroscopic technique. The methodology described herein will be used in the incorporation of other modifications into oligonucleotides of RNA, thus opening the possibility for a variety of novel modifications with potential reactivity that may lead to novel structural motifs with potential applications in nanomaterials and as agents in the control of biochemical structure and function. Furthermore, the described modeling is expected to guide efforts in the selection of groups whose reactivity and properties can result in the development of functional strands of RNA with distinct biophysical, photophysical, and chemical properties.

EXPERIMENTAL SECTION

General Methods. ^{1}H NMR, ^{13}C NMR, and ^{31}P NMR spectra were recorded at 300, 75, and 121.5 MHz, respectively. IR spectra were recorded on a diamond ATR sampler using powders of pure materials. Mass spectra (MALDI-TOF MS) for all the oligonucleotides were prepared as described elsewhere using a 2,4,6-trihydroxyacetophenone (THAP) matrix.[55] Pyridine, methylene chloride, dimethyl sulfoxide and Hunig's base were distilled over calcium hydride. Tetrahydrofuran was distilled over sodium and benzophenone. All other reagents were used as purchased without further purification. All intermediates and compounds analyzed for HRMS were carried out via ESI/APCI.

RNA Synthesis. Oligonucleotides were synthesized on CPG supports using C2′-*O*-TBDMS phosphoramidites. 0.25 M 5-Ethylthio-1*H*-tetrazole in acetonitrile was used as the coupling reagent, 3% dichloroacetic acid in dichloromethane was used for cleavage of the trityl group, a 2,6-lutidine/acetic anhydride solution was used for capping, and an I_2/THF/pyridine solution was used in the oxidation step. Coupling times of 10 min were used, with observed yields >97% for all modified phosphoramidites. Oligonucleotides were deacetylated/debenzoylated and cleaved from the CPG support in the presence of 1:1 aq. methylamine (40%) and aq. ammonia (40%) with heat (60 °C, 1.5 h). A mixture of *N*-methylpyrrolidinone/trimethylamine/HF (3:2:1) was used for deprotection of the TBDMS groups followed by purification via electrophoresis (20% denaturing PAGE). C_{18} columns were used to desalt the purified oligomers and eluted with 5 mM NH_4OAc. Oligonucleotides were redissolved in H_2O and used as obtained for subsequent experiments.

UV−Vis Spectroscopy. Concentrations of all oligonucleotides were calculated via UV−vis using a 1 mm path length with 1 μL volumes. Extinction coefficients for monomers were obtained in the same manner by dissolving the compounds of interest in water. Spectra corresponding to single stranded samples of **9**−**17** were carried out by preparing solutions of each oligonucleotide (30 μM) in 5 mM $MgCl_2$, 10 mM NaCl, 1 mM sodium phosphate adjusted to pH 7.3. Spectra corresponding to duplex samples were obtained by mixing both strands of interest in a 1:1 ratio followed by heat to 90 °C with slow cooling to room temperature. Origin 9.1 was used to normalize spectra of monomers and oligonucleotides for comparison.

CD Spectroscopy. CD spectra were recorded at various temperatures (PTC-348W1 Peltier thermostat) using Quartz cuvettes with a 1 cm path length. Spectra were averaged over three scans (350−200 nm, 0.5 nm intervals, 1 nm bandwidth, 1 s response time) and background corrected with the appropriate buffer or solvent. Solutions containing the RNA strands had the following composition: 2.5 μM RNA, 5 mM $MgCl_2$, 10 mM NaCl, 1 mM sodium phosphate-pH 7.3. All solutions prepared to record melting temperatures were hybridized prior to recording spectra by heating to 90 °C followed by slow cooling to room temperature. Melting temperatures were recorded at 210 nm with a ramp of 1°/min and step size of 0.2 with temperature ranges from 4 to 95 °C. A thin layer of mineral oil was added on top of each solution to keep concentrations constant at high temperatures. Origin 9.1 was used to determine all T_m values and to normalize CD spectra of ss-RNA and ds-oligonucleotides for both homo- and heteroduplexes.

*N-2-Acetyl-5′-O-[4,4′-dimethoxytrityl)-2′-O-(methylthiophene)-guanosine/N-2-Acetyl-5′-O-[4,4′-dimethoxytrityl)-3′-O-(methylthiophene)-guanosine (**6-G/7-G**).* A flask containing 7 g (11.2 mmol) of guanosine derivative **2**[56] was charged with dry DMSO (17 mL). In a separate flask, 5.18 g of KH (35% w/v suspension in oil, 44.8 mmol) was stirred vigorously in hexanes for 5 min; the volatile solvent was then removed via syringe followed by removal of volatiles under vacuum. The remaining gray powder was resuspended in dry THF (100 mL). The gray suspension was then cooled to 0 °C followed by addition of the DMSO solution over 20 min with evolution of gas. The solution was stirred for 2 h followed by dropwise addition of a solution containing 2-chloromethyl thiophene (1.35 mL, 12.3 mmol) in DMSO (17 mL). The resulting solution was then heated to 55 °C and stirred for additional 2.5 h. The reaction mixture was quenched using 20% aq, ammonium chloride (150 mL) and partitioned with the addition of EtOAc (100 mL). Organic residues were then washed with water (2 × 75 mL), brine (1 × 100 mL), and dried over anhydrous sodium sulfate. The organics were concentrated under reduced pressure resulting in a yellow oil. Purification via flash chromatography (DCM: EtOAc 20−40% EtOAc gradient), yielded 2.2 g (3 mmol, 26.8% yield) of modified nucleoside **6-G** in the form of a white foam. Overall, this material corresponded to the second fraction, with the first fraction corresponding to bis-addition products (not isolated). An additional 1 g (1.4 mmol, 12.5% yield) was obtained from a second column carried out on mixed fractions. ^{1}H NMR ($CDCl_3$) δ 11.84 (s, 1H), 8.26 (s, 1H), 8.26 (s, 1H), 7.51 (d, 1H) 7.49 (d, 1H), 7.38−7.33 (m, 4H), 7.24−7.21 (m, 3H), 6.86−6.77 (m, 7H), 5.87 (d, 1H), 4.90 (t, 1H), 4.85−4.75 (q, 2H), 4.43 (t, 1H), 4.21 (ddd, 1H), 3.78 (s, 3H), 3.76 (s, 3H), 3.54−3.50 (dd, 1H), 3.17−3.13 (dd, 1H), 2.91 (s, 1H), 1.61 (s, 3H); ^{13}C NMR ($CDCl_3$) δ 172.4, 171.2, 158.6, 155.8, 148.4, 147.5, 144.8, 139.4, 135.8, 135.6, 130, 128.1, 127.9. 126.9, 127, 126.8, 121.5, 113.2, 86.5, 84.5, 80.3, 69.8, 67.2, 60.4, 55.2, 23.9, 21.1, and 14.2; IR (ν/cm^{-1}) 2,930, 1,674, 1,606 and 1,560; HRMS, *m*/*z* calculated for $C_{38}H_{38}N_5O_8S$ $[M + H]^+$ 724.2441, obtained 724.2441.

Collection of the third fraction resulted in a white foam that corresponded to the C3′-*O*-regioisomer **7-G** (1.2 g, 16.6% containing impurities). ^{1}H NMR ($CDCl_3$) δ 11.79 (s, 1H), 7.97 (s, 1H), 7.76 (s, 1H), 7.53 (dd, 1H), 7.51 (dd, 1H), 7.40−7.36 (m, 4H), 7.24−7.21 (m, 3H), 6.89−6.80 (m, 7H), 5.75 (d, 1H), 5.22−5.16 (ddd, 1H), 4.94−4.77 (q, 2H), 4.70 (d, 1H), 4.34 (dd, 1H), 4.17 (ddd, 1H), 3.79 (s,

DOI: 10.1021/acs.joc.6b01615
J. Org. Chem. 2016, 81, 8947−8958

1H), 3.78 (s, 3H), 3.47 (dd, 1H), 2.95 (dd, 1H); HRMS, *m/z* calculated for $C_{38}H_{38}N_5O_8S$ $[M + H]^+$ 724.2441, obtained 724.2467.

*3′-O-(2-Cyanoethoxy-N,N-diisopropylaminophosphinyl)-N-2-acetyl-5′-O-[4,4′-dimethoxytrityl)-2′-O-(methylthiophene)-guanosine (**8-G**).* Nucleoside **6-G** (0.2 g, 0.28 mmol) was azeotropically dried over pyridine (2 mL) and resuspended in DCM (0.7 mL) and DIPEA (150 μL). 2-Cyanoethyl-*N,N′*-diisopropylchlorophosphoramidite (0.14 g, 0.59 mmol) was added dropwise and the solution was allowed to stir for 2 h. The reaction mixture was quenched with addition of aq. $NaHCO_3$ (20%) and extracted using DCM. The organic residues were then washed with H_2O (1 × 2 mL), brine (1 × 2 mL), and dried over anhydrous sodium sulfate. The organics were concentrated under reduced pressure and purified via flash chromatography (SiO_2, 20−40% EtOAc in DCM) yielded phosphoramidite **8**-G in the form of a white foam (0.18g, 0.2 mmol, 70%). ^{1}H NMR ($CDCl_3$) δ 11.8 (s, 1H), 8.24 (s, 1H), 8.04 (s, 1H), 7.64−7.21 (m, 10H), 6.9−6.78 (m, 6H), 5.94−5.77 (m, 1H), 4.94−4.57 (m, 3H), 4.24−3.93 (m, 2H), 3.8 (s, 6H), 3.59−3.21 (m, 5H), 2.8−2.65 (m, 4H), 2,2 (s, 6H), and 1.29−1.22 (m, 12H); ^{31}P NMR ($CDCl_3$) δ 150.1 and 149.3; HRMS, *m/z* calculated for $C_{47}H_{55}N_7O_9PS$ $[M + H]^+$ 924.3519, obtained 924.3517.

*N-6-Benzoyl-5′-O-[4,4′-dimethoxytrityl)-2′-O-(methylthiophene)-adenosine/N-6-Benzoyl-5′-O-[4,4′-dimethoxytrityl)-3′-O-(methylthiophene)-adenosine (**6-A/7-A**).* A round-bottom flask was charged with protected nucleoside **1**[57] (4.27 g, 6.34 mmol) and dissolved in a THF/DMSO solution (3:1, 37 mL). The solution was cooled (−78 °C) followed by addition of LiHMDS (16.5 mL, 1 M soln in hexanes) with stirring at this temperature for 1h. The solution was then warmed to rt and stirred for additional 2 h. and cooled down to −78 °C. A solution of 2-chloromethylthiophene in THF/DMSO (3:1 ratio, 37 mL) was then added and stirred for 12 h with warming to room temperature. A solution of aq. NH_4Cl was added (10 mM, 100 mL) followed by washing of the organic residues with brine (75 mL) and drying over anhydrous sodium sulfate. The organic residues were concentrated under reduced pressure and purified via column flash chromatography (SiO_2, 1:1 EtOAc/hexanes followed by gradient to 4:1 EtOAc/hexanes) to yield 0.72 g (0.93 mmol, 14.8%) of modified nucleoside **6-A** in the form of a white foam. This material corresponded to the second fraction, with the first fraction corresponding to bis-addition products (not isolated). ^{1}H NMR ($CDCl_3$) δ 9.13 (s, 1H), 8.74 (s, 1H), 8.12 (s, 1H), 8.02 (d, *J* = 4.0 Hz, 2H), 7.61−7.58 (m, 1H), 7.53−7.49 (m, 2H) 7.41 (d, *J* = 8 Hz, 2H) 7.31−7.18 (m, 7H), 6.89 (d, *J* = 4 Hz, 1H), 6.85−6.83 (m, 1H), 6.80 (d, 4H), 6.18 (d, *J* = 4.0 Hz, 1H), 4.91 (d, 2H), 4.75 (t, 1H), 4.41 (d, *J* = 4.0 Hz, 1H), 4.24 (t, 1H), 3.77 (s, 6H), 3.52−3.35 (m, 2H), 2.93 (d, *J* = 4 Hz, 1H); ^{13}C NMR ($CDCl_3$) δ 164.8, 158.8, 157.8, 152.9,151.5, 149.7, 144.7, 141.9, 139.2, 135.9, 135.9, 135.8, 133.9, 133, 130.5, 130.3, 130.3, 128.1, 128.1, 127.4, 127.1, 123.7, 113.4, 87.4, 86.8, 84.5, 80.4, 77.6, 77.3, 77, 70.8, 70.1, 67.5, 63.1, 55.5; IR (ν/cm^{-1}) 3283, 3058, 2931, 2828, 1726, and 1703; HRMS, *m/z* calculated for $C_{43}H_{40}N_5O_7S$ $[M + H]^+$ 770.2648, obtained 770.2665.

Collection of the third fraction resulted in a white foam that corresponded to the C3′-*O*-regioisomer **7-A** (0.16 g, 0.21 mmol, 3.3%). ^{1}H NMR ($CDCl_3$) δ 8.92 (s, 1H), 8.76 (s, 1H), 8.19 (s, 1H), 8.03 (d, *J* = 4.0 Hz, 2H), 7.63−7.60 (m, 1H), 7.55−7.51 (m, 2H) 7.36−7.20 (m, 12H), 6.97−6.94(m, 2H), 6.80 (d, 4H), 6.06 (d, *J* = 8.0 Hz, 1H), 4.87−4.83 (m, 3H), 4.44−4.42 (t, 1H), 4.31 (d, *J* = 4.0 Hz, 1H), 3.78 (s, 6H), 3.53 (d, *J* = 8 Hz, 1H), 3.45−3.22 (dd, *J* = 4.0 Hz, 2H); ^{13}C NMR ($CDCl_3$) δ 164.8, 158.8, 152.8, 149.8, 144.6, 142, 139.6, 135.8, 135.7,133.8, 133, 130.2, 128.1, 127.1, 127.1, 113.4, 89.7, 86.8, 82.8, 77.6, 77.3, 77, 74.2, 67.3, 65.9, 63.1, 60.6, 55.5; HRMS, *m/z* calculated for $C_{43}H_{40}N_5O_7S$ $[M + H]^+$ 770.2648, obtained 770.2642.

*3′-O-(2-Cyanoethoxy-N,N-diisopropylaminophosphinyl)-N-6-benzoyl-5′-O-[4,4′-dimethoxytrityl)-2′-O-(methylthiophene)-adenosine (**8-A**).* Nucleoside **6-A** (0.2 g, 0.26 mmol) was dissolved in DCM (1.5 mL) and DIPEA (0.11 g, 0.85 mmol) followed by dropwise addition of 2-cyanoethyl-*N,N′*-diisopropylchlorophosphoramidite (0.09 g, 0.38 mmol) was added dropwise and stirred for 75 min. The reaction mixture was quenched using aq. $NaHCO_3$ (20%) and partitioned with DCM. The organic residues were then washed with H_2O (1 × 2 mL), brine (1 × 2 mL), and dried over anhydrous sodium sulfate. The organics were concentrated under reduced pressure and purified via flash chromatography (SiO_2, EtOAc/hexanes 2:3 × 2, then 1:1 EtOAc/hexanes) yielded phosphoramidite **8**-A in the form of a white foam (0.19g, 0.2 mmol, 77%). ^{1}H NMR ($CDCl_3$) δ 8.94 (s, 1H), 8.67−8.66 (m, 1H), 8.06−8.02 (m, 4H), 7.62 (m, 1H), 7.53 (m, 2H), 7.40 (m, 2H) 7.31−7.15 (m, 7H) 6.88−6.78 (m, 4H), 6.14−6.11 (m, 1H), 4.98−4.88 (m, 2H), 4.74−4.61 (m, 2H), 4.42−4.37 (m, 1H), 3.91−3.55 (m, 12H), 3.59−3.31 (m, 1H), 2.61−2.53 (m, 2H), 2.41−2.37 (m, 1H), 1.67 (m, 2H), 1.31−1.10 (m, 17H); ^{31}P NMR ($CDCl_3$) δ 150.7, 150.1; HRMS, *m/z* calculated for $C_{52}H_{57}N_7O_8PS$ $[M + H]^+$ 970.3727, obtained 970.3747.

*N-4-Acetyl-5′-O-(4,4′-dimethoxytrityl)-2′-O-(methylthiophene)-cytidine/N-4-Acetyl-5′-O-(4,4′-dimethoxytrityl)-3′-O-(methylthiophene)-cytidine (**6-C/7-C**).* Nucleoside **3**[58] (2 g, 3.4 mmol) was added to a flame-dried 50 mL round-bottom flask, equipped with a magnetic stirrer, and dissolved in an anhydrous THF/DMSO solution (12/8 mL). The solution was cooled to −78 °C followed by addition of LiHMDS (7.5 mL, 1 M in hexanes) and stirring while warming to rt over 0.5 h. The solution was cooled back to −78 °C followed by addition of a solution of 2-chloromethylthiophene (1 g, 7.5 mmol in THF/DMSO, 1:1, 1 mL). The reaction mixture was warmed to room temperature over 30 min and heated to 55 °C with stirring for 5 h followed by additional stirring at room temperature for 12 h. The suspension was quenched with aq. NH_4Cl (10 mM, 50 mL) and partitioned using EtOAc. The organics were washed with brine (40 mL), dried over anhydrous sodium sulfate, and concentrated under reduced pressure. The remainders were purified via flash column chromatography (SiO_2, 3:2 EtOAc/Hexanes) to yield modified nucleoside **6-C** in the form of yellow foam (First fraction: 0.151 g, 0.22 mmol, 6.5%). ^{1}H NMR ($CDCl_3$) δ 8.84 (s, 1H), 8.33 (d, *J* = 9, 1H), 7.45−7.23 (m, 9H), 7.14 (m, 1H), 7.00 (m, 2H), 6.98 (d, 1H), 6.89 (m, 4H), 5.93 (s, 1H), 5.09 (s, 2H), 4.36 (m, 1H), 4.05 (m, 2H), 3.78 (s, 6H), 3.41 (m, 2H), 3.12 (d, *J* = 9, 1H), 2.12 (s, 3H); ^{13}C NMR ($CDCl_3$) δ 170.6, 163, 158.7, 155, 144.9, 144.3, 139.7, 135.5, 135.3, 130.1, 128.1, 128, 126.9, 113.4, 96.8, 88.9, 87.1, 83.3, 80.7, 67.6, 66.6, 60.9, 55.3, and 24.9; IR (neat, ν/cm^{-1}) 3068.09, 2929.84, 2835.44, 1719.19. HRMS, *m/z* calculated for $C_{37}H_{38}N_3O_8S$ $[M + H]^+$ 684.2374, obtained 684.2379.

Collection of a second fraction resulted in a white foam that corresponded to the C3′-*O*-regioisomer **7-C** (0.47 g, 0.67 mmol, 20%). ^{1}H NMR ($CDCl_3$) δ 10.88 (s, 1H), 8.32(d, *J* = 9, 1H), 7.49 (d, *J* = 3, 1H) 7.31−7.12 (m, 9H), 7.05 (s, 1H), 7.00−6.92 (m, 2H), 6.89−6.86 (m, 4H) 5.78 (s, 1H), 5.71 (d, *J* = 6, 1H), 4.80 (d, *J* = 12, 1H), 4.66 (d, *J* = 12, 1H), 4.33 (s, 1H), 4.25−4.21 (m, 1H), 4.15 (m, 1H), 3.74 (s, 6H), 3.32 (m, 2H), 2.09 (s, 3H); ^{13}C NMR ($CDCl_3$) 171.3, 163.1, 159.3, 155.9, 145.4, 145, 140.7, 136.1, 135, 130.6, 128.7, 128.5, 127.4, 127.1, 117.9, 113.7, 96.2, 92.1, 92.6, 87.2, 81.3, 75.2, 73.4, 86.6, 61.6, 55.5, and 24.6; IR (ν/cm^{-1}) 3236.64, 3067.73, 2930.12, 2832.81, 1719.27. HRMS, *m/z* calculated for $C_{37}H_{37}N_3O_8NaS$ $[M + Na]^+$ 706.2199, obtained 706.2212.

*3′-O-(2-Cyanoethoxy-N,N-diisopropylaminophosphinyl)-N-4-acetyl-5′-O-[4,4′-dimethoxytrityl)-2′-O-(2-methylthiophene)-cytidine (**8-C**).* Nucleoside **6-C** (0.255 g, 0.37 mmol) was added into a 10 mL flame-dried round-bottom flask and azeotropically dried over pyridine (1 mL). The obtained foam was redissolved in DCM (1.5 mL) and DIPEA (0.33 g, 2.6 mmol) followed by dropwise addition of 2-cyanoethyl-*N,N′*-diisopropylchlorophosphoramidite (0.13 g, 0.55 mmol) and stirring of the suspension for 1 h. An aq. $NaHCO_3$ solution (2 mL, 10%) was added and the organics were extracted over DCM (5 mL), washed with brine (1 × 5 mL), dried over anhydrous sodium sulfate, and concentrated under reduced pressure. Purification of the organic residues was achieved via flash column chromatography (EtOAc/Hexanes, gradient from 60% to 100% EtOAc) to afford phosphoramidite **8-C** in the form of a white foam (0.23 g, 0.26 mmol, 70%). ^{1}H NMR ($CDCl_3$) δ 9.13−9.04 (m 1H), 8.58−8.46 (m, 1H) 7.44−6.82 (m, 17H), 6.07 (m, 1H), 5.20−4.96 (m, 2H), 4.59−4.05 (m, 3H), 3.81 (m, 6H), 3.78−3.35 (m, 6H), 2.42−2.04 (m, 5H) 1.63−0.95 (m, 12H); ^{31}P NMR (120 MHz, $CDCl_3$) δ 149.87; IR (ν/cm^{-1})

DOI: 10.1021/acs.joc.6b01615
J. Org. Chem. 2016, 81, 8947−8958

3071.61, 2929.82, 2871.64, 1719.65. HRMS, *m/z* calculated for $C_{46}H_{54}N_5O_9NaPS$ 906.3278 $[M + Na]^+$, calcd 906.3272.

C3′,C5′-Diterbutylsilyl-C2′-O-(2-methylthiophene)-uridine 4′. Nucleoside **4**[59] (2.1 g, 5.4 mmol) was added to a 100 mL flask and dissolved in anhydrous THF (45 mL). The flask was cooled to −78 °C, followed by the addition of a 1.0 M sodium bis(trimethylsilyl)-amide solution (10.9 mL, 10.9 mmol in THF). The mixture was stirred under an argon atmosphere for 25 min before the flask was removed from the bath and allowed to return to rt over 30 min. A solution of DMSO containing 2-chloromethylthiophene (0.67 mL, 6.3 mmol in 15 mL) was added to the flask dropwise over 3 min. The reaction was stirred for 18 h before addition of an aq. solution (0.1 M NH_4Cl, 50 mL) and extractions over EtOAc (3 × 20 mL). The organic content was washed with brine (1 × 35 mL), dried over anhydrous sodium sulfate, and concentrated under reduced pressure. The remainder oil was purified via flash column chromatography (SiO_2, EtOAc:Hexanes gradient from 25% to 33% EtOAc) to afford modified nucleoside **4′** in the form of a yellow foam (1.15 g, 2.4 mmol, 45%). δ 8.54 (s, 1H), 7.33−7.21 (m, 2H), 7.06−7.05 (m, 1H), 6.99−6.94 (m, 1H), 5.75−5.71 (m, 1H), 5.67 (s, 1H), 5.15−4.95 (m, 2H), 4.51−4.45 (m, 1H), 4.21−3.95 (m, 4H), and 1.10−1.03 (m, 18H); ^{13}C NMR (75 MHz, $CDCl_3$) δ 163.4, 149.8, 140.5, 140.1, 126.6, 126.5, 126, 102.5, 92.2, 79.7, 77.5, 76.6, 74.7, 67.6, 67.3, 60.4, 27.4, 27.1, 22.8, 21.1, 20.4, 14.2; IR (ν/cm^{-1}) 3055.74, 2933.57, 2858.11, and 1682.23. HRMS *m/z* calculated for $C_{22}H_{33}N_2O_6SiS$ $[M + H]^+$ = 481.1829, observed *m/z* = 481.1831.

*2-Methylthiophen-yl-uridine **5***. Nucleoside **4′** (0.72 g, 1.5 mmol) was added to a 10 mL flask and dissolved in anhydrous THF (5.5 mL). A solution of 3HF·Et_3N (1.25 mL, 7.44 mmol) in pyr. (1.9 mL) was added to the flask and stirred for 2h. Sodium bicarbonate (1.87 g, 22.3 mol) was then added at once followed by addition of H_2O (3 mL) to observe the evolution of gas. The organics were concentrated under reduced pressure and purified via flash column chromatography (MeOH:DCM gradient from 0.1% to 8% MeOH) to afford diol **5** in the form of a white foam (0.32 g, 0.96 mmol, 62%). ^1H NMR (300 MHz, DMSO) δ 11.32 (s, 1H), 7.82 (d, *J* = 9 Hz, 1H), 7.48−7.46 (m, 1H), 7.05−7.04 (m, 1H), 6.98−6.95 (m, 1H), 5.90 (d, *J* = 6 Hz, 1H), 5.58 (d, *J* = 9 Hz, 1H), 5.22 (d, *J* = 6 Hz, 1H), 5.14−5.11 (m, 1H), 4.79 (dd, *J* = 12 Hz, 39 Hz, 2H), 4.14 (q, *J* = 6 Hz, 9 Hz, 1H), 4.02−3.99 (m, 1H), 3.91−3.88 (m, 1H), 3.67−and 3.52 (m, 2H); ^{13}C NMR (75 MHz, DMSO) δ 163.5, 151, 141, 140.7, 127.3, 127.1, 127, 102.3, 86.5, 85.8, 80.4, 68.8, 66.1, and 61; IR (ν/cm^{-1}) 3056.80, 2933.65, 2858.52, and 1681.92. HRMS *m/z* calculated for $C_{14}H_{16}N_2O_6NaS$ $[M + Na]^+$ = 363.0627, observed *m/z* = 363.0629.

*5′-O-[4,4′-Dimethoxytrityl)-3′-O-(methylthiophene)-uridine (**6-U**)*. Nucleoside **5** (0.16 g, 0.47 mmol) was azeotropically dried over anhydrous pyridine (2 × 1 mL) followed by the addition of anhydrous pyr. (2.5 mL) and cooling to 0 °C. DMTrCl (0.18 g, 0.525 mmol) was added to the flask and stirred with warming to room temperature over 8 h. An aq. $NaHCO_3$ solution (20%, 50 mL) was added followed by extractions over EtOAc (3 × 20 mL), washed with brine (1 × 30 mL), and dried over anhydrous sodium sulfate. The organic residues were concentrated under reduced pressure and purified via flash column chromatography (SiO_2, MeOH:DCM gradient from 0% to 4% MeOH) to afford nucleoside **6-U** in the form of a white foam (0.27 g, 0.43 mmol, 90.7%). ^1H NMR (300 MHz, $CDCl_3$) δ 8.56 (s, 1H), 7.98 (d, *J* = 6 Hz, 1H), 7.38−7.23 (m, 10H), 7.08−7.07 (m, 1H), 7.00−6.97 (m, 1H), 6.86−6.81 (m, 4H), 6.02 (d, *J* = 3 Hz, 1H), 5.25 (d, *J* = 9 Hz, 1H), 5.10−4.97 (m, 2H), 4.46−4.38 (m, 1H), 4.08−4.03 (m, 2H), 3.80 (s, 6H), 3.56−3.47 (m, 2H), and 2.56 (d, *J* = 9 Hz, 1H); ^{13}C NMR (75 MHz, $CDCl_3$) δ 163.6, 158.7, 158.7, 150.3, 144.4, 140, 139.4, 135.3, 135.1, 130.2, 130.1, 128.1, 128, 128, 127.2, 127, 126.9, 113.3, 102.1, 87.5, 87.1, 83.5, 80.7, 77.5, 77.1, 76.7, 68.4, 66.7, 61.3, 55.3, and 31; IR (ν/cm^{-1}) 3056.01, 2933.41, and 1674.92. HRMS *m/z* calculated for $C_{35}H_{34}N_2O_8NaS$ $[M + Na]^+$ = 665.1934, observed *m/z* = 665.1942.

*3′-O-(2-Cyanoethoxy-N,N-diisopropylaminophosphinyl)-5′-O-[4,4′-dimethoxytrityl)-2′-O-(2-methylthiophene)-uridine (**8-U**)*. Nucleoside **6-U** (0.2 g, 0.32 mmol) was added to a 5 mL round-bottom flask and dissolved in DCM (1 mL) and DIPEA (0.15 g, 1.15 mmol). *N,N*-Diisopropylamino-cyanoethyl-phosphonamidic chloride (1.3 g, 0.55 mmol) was added and stirred for 110 min before addition of an aq. NaHCO3 solution (20%, 2 mL). The aqueous layer was extracted with DCM (2 × 10 mL), washed with brine, and dried over anhydrous sodium sulfate. The organic residues were concentrated under reduced pressure and purified via flash column chromatography (SiO_2, EtOAc:Hexanes gradient from 0% to 66% EtOAc) to afford phosphoramidite **8-U** in the form of a white foam (0.2 g, 0.25 mmol, 81.4%). ^1H NMR (300 MHz, $CDCl_3$) δ 8.24 (s, 1H), 7.93−7.84 (m, 1H), 7.39−7.22 (m, 10H), 7.07−7.03 (m, 1H), 6.98−6.93 (m, 1H), 6.85−6.79 (m, 4H), 6.08−6.03 (m, 1H), 5.22−5.16 (m, 1H), 4.94 (s, 2H), 4.60−4.45 (m, 1H), 4.30−4.17 (m, 2H), 3.80−3.79 (m, 6H), 3.75−3.38 (m, 6H), 2.63−2.41 (m, 2H), and 1.18−1.02 (m, 12H); ^{31}P NMR (120 MHz, $CDCl_3$) δ 150.11; IR (ν/cm^{-1}) 3056.72, 2965.50, and 1682.35. HRMS *m/z* calculated for $C_{44}H_{52}N_4O_9PS$ $[M + H]^+$ = 843.3193, observed *m/z* = 843.3197.

■ ASSOCIATED CONTENT

Supporting Information

The Supporting Information is available free of charge on the ACS Publications website at DOI: 10.1021/acs.joc.6b01615.

NMR, IR, and MS spectra corresponding to the characterization of the described compounds; CD spectra of all the pertinent experiments, including melting temperature measurements and van't Hoff plots; Tables that include the atom coordinates and absolute energies corresponding to the theoretical calculations for **18**:**19** and **20**:**21** (PDF)

Structure data (XYZ)

Structure data (XYZ)

■ AUTHOR INFORMATION

Corresponding Author

*E-mail: marino.resendiz@ucdenver.edu.

Notes

The authors declare no competing financial interest.

■ ACKNOWLEDGMENTS

This work was supported via start-up funds, CU Denver. J.C.N. and J.T. would like to acknowledge a Research and Creative Activities Award (RaCAS, CU Denver) for support. H.W. acknowledges the support from the National Science Foundation CHE-1500285. This research has used resources of the National Energy Research Scientific Computing Center, a DOE Office of Science User Facility supported by the Office of Science of the U.S. Department of Energy under Contract No. DE-AC02-05CH11231. We thank the University of Colorado Denver for support in the purchase of the CD spectrometer. Mass spectrometry of oligonucleotides was carried out at the mass spectrometry core facilities, University of Colorado Skaggs School of Pharmacy and Pharmaceutical Sciences, Anschutz Medical Campus.

■ REFERENCES

(1) Seeman, N. C. *Annu. Rev. Biochem.* **2010**, *79*, 65−87.
(2) Deleavey, G. F.; Damha, M. J. *Chem. Biol.* **2012**, *19*, 937−954.
(3) Wachowius, F.; Höbartner. *ChemBioChem* **2010**, *11*, 469−480.
(4) Dai, N.; Kool, E. T. *Chem. Soc. Rev.* **2011**, *40*, 5756−5770.
(5) Nakamura, M.; Ohtoshi, Y.; Yamana, K. *Chem. Commun.* **2005**, 5163−5165.
(6) Nguyen, P.; Qin, P. Z. *WIREs RNA* **2012**, *3*, 67−72.
(7) Tanpure, A. A.; Pawar, M. G.; Srivatsan, S. G. *Isr. J. Chem.* **2013**, *53*, 366−378.
(8) Tinsley, R. A.; Walter, N. G. *RNA* **2006**, *12*, 522−529.

DOI: 10.1021/acs.joc.6b01615
J. Org. Chem. 2016, 81, 8947−8958

(9) Höbartner, C.; Sicoli, G.; Wachowius, F.; Gophane, D. B.; Sigurdsson, S. T. *J. Org. Chem.* **2012**, *77*, 7749−7754.
(10) Chalmers, B. A.; Saha, S.; Nguyen, T.; McMurtrie, J.; Sigurdsson, S. T.; Bottle, S. E.; Masters, K.-S. *Org. Lett.* **2014**, *16*, 5528−5531.
(11) Kumar, P.; Shaikh, K. I.; Jørgensen, A. S.; Kumar, S.; Nielsen, P. *J. Org. Chem.* **2012**, *77*, 9562−9573.
(12) Karmakar, S.; Guenther, D. C.; Hrdlicka, P. J. *J. Org. Chem.* **2013**, *78*, 12040−12048.
(13) Majlessi, M.; Nelson, N. C.; Becker, M. M. *Nucleic Acids Res.* **1998**, *26*, 2224−2229.
(14) Yamada, T.; Okaniwa, N.; Saneyoshi, H.; Ohkubo, A.; Seio, K.; Nagata, T.; Aoki, Y.; Takeda, S.; Sekine, M. *J. Org. Chem.* **2011**, *76*, 3042−3053.
(15) Saito, Y.; Hashimoto, Y.; Arai, M.; Tarashima, N.; Miyazawa, T.; Miki, K.; Takahashi, M.; Furukawa, K.; Yamazaki, N.; Matsuda, A.; Ishida, T.; Minakawa, N. *ChemBioChem* **2014**, *15*, 2535−2540.
(16) Blechinger, J.; Pieper, H.; Marzenell, P.; Kovbasyuk, L.; Serva, A.; Starkuviene, V.; Erfle, H.; Mokhir, A. *Chem. Commun.* **2013**, *49*, 7397−7399.
(17) Østergaard, M. E.; Cheguru, P.; Papasani, M. R.; Hill, R. A.; Hrdlicka, P. J. *J. Am. Chem. Soc.* **2010**, *132*, 14221−14228.
(18) Krasheninina, O. A.; Novopashina, D. S.; Lomzov, A. A.; Venyaminova, A. G. *ChemBioChem* **2014**, *15*, 1939−1946.
(19) Gupta, P.; Langkjaer, N.; Wengel, J. *Bioconjugate Chem.* **2010**, *21*, 513−520.
(20) Osawa, T.; Hari, Y.; Dohi, M.; Matsuda, Y.; Obika, S. *J. Org. Chem.* **2015**, *80*, 10474−10481.
(21) Noé, M. S.; Sinkeldam, R. W.; Tor, Y. *J. Org. Chem.* **2013**, *78*, 8123−8128.
(22) Wicke, L.; Engels, J. W. *Bioconjugate Chem.* **2012**, *23*, 627−642.
(23) Srivatsan, S. G.; Tor, Y. *Chem. - Asian J.* **2009**, *4*, 419−427.
(24) Pawar, M. G.; Srivatsan, S. G. *Org. Lett.* **2011**, *13*, 1114−1117.
(25) Ghodke, P. P.; Gore, K. R.; Harikrishna, S.; Samanta, B.; Kottur, J.; Nair, D. T.; Pradeepkumar, P. I. *J. Org. Chem.* **2016**, *81*, 502−511.
(26) Wicke, L.; Engels, J. W. *Bioconjugate Chem.* **2012**, *23*, 627−642.
(27) Resendiz, M. J. E.; Taing, J.; Khan, S. I.; Garcia-Garibay, M. A. *J. Org. Chem.* **2008**, *73*, 638−643.
(28) Chaulk, S. G.; MacMillan, A. M. *Nat. Protoc.* **2007**, *2*, 1052−1058.
(29) Ohtsuka, E.; Tanaka, S.; Ikehara, M. *Chem. Pharm. Bull.* **1977**, *25*, 949−959.
(30) Huynh, H. V.; Chew, Y. X. *Inorg. Chim. Acta* **2010**, *363*, 1979−1983.
(31) ^{1}H-NMR spectrum of thiophene-2-methylchloride was in agreement with the literature: Davis, C. M. *Synth. Commun.* **2005**, *35*, 2079−2083. This material was synthesized in <1 mmol batches and stored in ampoules under an inert atmosphere. Larger scale synthesis and storage in larger containers resulted in the development of impurities (color change) over time that then led to decomposition in a highly exothermic reaction.
(32) Chaulk, S. G.; MacMillan, A. M. *Nucleic Acids Res.* **1998**, *26*, 3173−3178.
(33) Cavaluzzi, M. J.; Borer, P. N. *Nucleic Acids Res.* **2004**, *32* (1), e13.
(34) Kypr, J.; Kejnovská, I.; Renčiuk, D.; Vorlíčková, M. *Nucleic Acids Res.* **2009**, *37*, 1713−1725.
(35) Chauca-Diaz, A. M.; Choi, Y. J.; Resendiz, M. J. E. *Biopolymers* **2015**, *103*, 167−174.
(36) Barbas, C. F.; Burton, D. R.; Silverman, G. J. *Cold Spring Harbor Protoc.* **2007**, *2007*, pdb.ip47.
(37) Keel, A. Y.; Jha, B. K.; Kieft, J. S. *RNA* **2012**, *18*, 88−99.
(38) Mikulecky, P. J.; Feig, A. L. *Biopolymers* **2006**, *82*, 38−58.
(39) Košutić, M.; Jud, L.; Da Veiga, C.; Frener, M.; Fauster, K.; Kreutz, C.; Ennifar, E.; Micura, R. *J. Am. Chem. Soc.* **2014**, *136*, 6656−6663.
(40) Frisch, M. J.; Trucks, G. W.; Schlegel, H. B.; Scuseria, G. E.; Robb, M. A.; Cheeseman, J. R.; Scalmani, G.; Barone, V.; Mennucci, B.; Petersson, G. A.; Nakatsuji, H.; Caricato, M.; Li, X.; Hratchian, H. P.; Izmaylov, A. F.; Bloino, J.; Zheng, G.; Sonnenberg, J. L.; Hada, M.; Ehara, M.; Toyota, K.; Fukuda, R.; Hasegawa, J.; Ishida, M.; Nakajima, T.; Honda, Y.; Kitao, O.; Nakai, H.; Vreven, T.; Montgomery, Jr., J. A.; Peralta, J. E.; Ogliaro, F.; Bearpark, M.; Heyd, J. J.; Brothers, E.; Kudin, K. N.; Staroverov, V. N.; Kobayashi, R.; Normand, J.; Raghavachari, K.; Rendell, A.; Burant, J. C.; Iyengar, S. S.; Tomasi, J.; Cossi, M.; Rega, N.; Millam, N. J.; Klene, M.; Knox, J. E.; Cross, J. B.; Bakken, V.; Adamo, C.; Jaramillo, J.; Gomperts, R.; Stratmann, R. E.; Yazyev, O.; Austin, A. J.; Cammi, R.; Pomelli, C.; Ochterski, J. W.; Martin, R. L.; Morokuma, K.; Zakrzewski, V. G.; Voth, G. A.; Salvador, P.; Dannenberg, J. J.; Dapprich, S.; Daniels, A. D.; Farkas, ö.; Foresman, J. B.; Ortiz, J. V.; Cioslowski, J.; Fox, D. J. *Gaussian 09*; Gaussian, Inc.: Wallingford, CT, 2009.
(41) Barone, V.; Cossi, M.; Tomasi, J. *J. Chem. Phys.* **1997**, *107*, 3210−3221.
(42) Cammi, R.; Mennucci, B.; Tomasi, J. *J. Phys. Chem. A* **1998**, *102*, 870−875.
(43) Cammi, R.; Mennucci, B.; Tomasi, J. *J. Phys. Chem. A* **2000**, *104*, 4690−4698.
(44) Altona, C.; Sundaralingam, M. *J. Am. Chem. Soc.* **1972**, *94*, 8205−8212.
(45) Clark, C. L.; Cecil, P. K.; Singh, D.; Gray, D. M. *Nucleic Acids Res.* **1997**, *25*, 4098−4105.
(46) Cheatham, T. E., III; Kollman, P. A. *J. Am. Chem. Soc.* **1997**, *119*, 4805−4825.
(47) Nakamura, M.; Fukunaga, Y.; Sasa, K.; Ohtoshi, Y.; Kanaori, K.; Hayashi, H.; Nakano, H.; Yamana, K. *Nucleic Acids Res.* **2005**, *33*, 5887−5895.
(48) Nakamura, M.; Shimomura, Y.; Ohtoshi, Y.; Sasa, K.; Hayashi, H.; Nakano, H.; Yamana, K. *Org. Biomol. Chem.* **2007**, *5*, 1945−1951.
(49) Anderson, B. A.; Hrdlicka, P. J. *J. Org. Chem.* **2016**, *81*, 3335.
(50) Nakamura, M.; Fukuca, M.; Takada, T.; Yamana, K. *Org. Biomol. Chem.* **2012**, *10*, 9620−9626.
(51) Nakamura, M.; Murakami, Y.; Sasa, K.; Hayashi, H.; Yamana, K. *J. Am. Chem. Soc.* **2008**, *130*, 6904−6905.
(52) Scott, J. F.; Zamecnik, P. C. *Proc. Natl. Acad. Sci. U. S. A.* **1969**, *64*, 1308−1314.
(53) Anosova, I.; Kowal, E. A.; Dunn, M. R.; Chaput, J. C.; Van Horn, W. D.; Egli, M. *Nucleic Acids Res.* **2016**, *44*, 1007−1021.
(54) Pallan, P. S.; Greene, E. M.; Jicman, P. A.; Pandey, R. K.; Manoharan, M.; Rozners, E.; Egli, M. *Nucleic Acids Res.* **2011**, *39*, 3482−3495.
(55) Chapman, E. G.; DeRose, V. J. *J. Am. Chem. Soc.* **2010**, *132*, 1946−1952.
(56) Pitsch, S.; Weiss, P. A.; Wu, X.; Ackermann, D.; Honegger, T. *Helv. Chim. Acta* **1999**, *82*, 1753−1761.
(57) Hevroni, B. L.; Sayer, A. H.; Blum, E.; Fischer, B. *Inorg. Chem.* **2014**, *53*, 1594−1605.
(58) Watanabe, K. A.; Fox, J. J. *Angew. Chem., Int. Ed. Engl.* **1996**, *5*, 579−580.
(59) Dai, Q.; Piccirilli, J. A. *Org. Lett.* **2003**, *5*, 807−810.

DOI: 10.1021/acs.joc.6b01615
J. Org. Chem. 2016, 81, 8947−8958